GeoHealth

Generation, Resuspension, and Transport of Particulate Matter From Biochar-Amended Soils: A Potential Health Risk

Sujith Ravi[1] (ID), Junran Li[2] (ID), Zhongju Meng[3], Jianguo Zhang[4], and Sanjay Mohanty[5] (ID)

[1]Department of Earth and Environmental Science, Temple University, Philadelphia, PA, USA, [2]Department of Geosciences, The University of Tulsa, Tulsa, OK, USA, [3]Desert Science and Engineering College, Inner Mongolia Agricultural University, Hohhot, China, [4]College of Natural Resources and Environment, Northwest A&F University, Shaanxi, China, [5]Department of Civil and Environmental Engineering, University of California, Los Angeles, CA, USA

Abstract Large-scale soil application of biochar is one of the terrestrial carbon sequestration strategies for future climate change mitigation pathways, which can also help remove and sequester pollutants from contaminated soil and water. However, black carbon emissions from biochar-amended soils can deteriorate air quality and affect human health, as the biochar particles often contain a higher amount of sorbed toxic pollutants than the soil. Yet, the extent and mechanism of inhalable particulate matter (PM_{10}) emission from biochar-amended soils at different wind regimes have not been evaluated. Using wind tunnel experiments to simulate different wind regimes, we quantified particulate emission from sand amended with 1–4% (by weight) biochar at two size fractions: with and without <2-mm biochar. At wind speeds below the threshold speed for soil erosion, biochar application significantly increased PM_{10} emission by up to 400% due to the direct resuspension of inhalable biochar particles. At wind speeds above the threshold speed, emission increased by up to 300% even from biochar without inhalable fractions due to collisions of fast-moving sand particles with large biochar particles. Using a theoretical framework, we show that particulate matter emissions from biochar-amended soils could be higher than that previously expected at wind speeds below the erosion threshold wind speed for background soil. Our results indicate that current models for fugitive dust emissions may underestimate the particulate matter emission potential of biochar-amended soils and will help improve the assessment of biochar emission from amended soils.

1. Introduction

Large-scale application of biochar—a carbonaceous porous material produced by pyrolysis of organic waste—provides several benefits including carbon sequestration (Lehmann, 2007; Smith, 2016), sustainable bioenergy production (Sohi, 2013), improvement of soil productivity (Lehmann et al., 2011), natural treatment of contaminated waters (Ulrich et al., 2015), and remediation of contaminated land (Cao et al., 2009). Biochar application, a negative CO_2 emission technology, has been recommended as an integral component of future climate change mitigation pathways (Lehmann, 2007). Optimistic scenarios for global biochar application estimate that up to 101.5 Pg C from biochar will be applied in 4.03 G ha of cropland and pastures in the next 100 years (Woolf et al., 2010).

The applied biochar is expected to remain in the soil for hundreds of years (Lehmann, 2015; Nguyen & Lehmann, 2009), thereby mitigating climate change impacts and slowing down land degradation (Mbow et al., 2019; United Nations Convention to Combat Desertification, 2009; Woolf et al., 2010). However, recent studies have shown that the applied biochar may also leave the application areas either by wind or water transport (Mohanty & Boehm, 2015; Ravi et al., 2016), thereby lowering their intended effect on improving soil or water quality. Because biochar particles often contain a higher amount of toxic pollutants than the soil in application areas (Mohanty & Boehm, 2015; Sasidharan et al., 2016), particulate matter emissions from biochar can deteriorate air quality and adversely affect human health (Genesio et al., 2016; Janssen et al., 2011). Further, black carbon emission may counteract the desired negative emission potential of biochar-based carbon sequestration programs (Genesio et al., 2016).

Although numerous studies (Ghavanloughajar et al., 2020; Lehmann, 2015; Mohanty & Boehm, 2015; Rumpel et al., 2009; Wang et al., 2013) have examined biochar erosion by water, far fewer studies
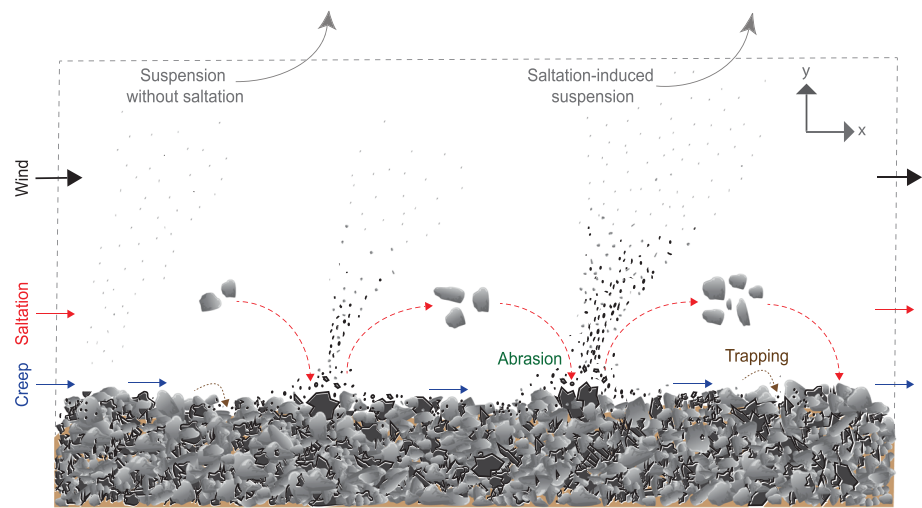
Figure 1. A conceptual framework of eolian erosion and transport processes within a two-dimensional control volume with biochar (black) and soil (gray) particles.

(Gelardi et al., 2019; Ravi et al., 2016) have evaluated biochar loss by the wind. A recent study (Ravi et al., 2016) provided evidence for increased particulate matter emissions in soils with increases in biochar fraction. The results show that the threshold velocity—the minimum velocity for wind erosion to occur—for biochar-amended soil could be lower than that of natural soil, indicating that emission potential is sensitive to wind conditions (Ravi et al., 2016). Wind conditions vary significantly over spatial and temporal scales, yet no study to date has examined biochar emission mechanisms and potential in entire wind regimes: pre-threshold, threshold, and post-threshold or abrasion phases. The previous study only accounted for the emission of fine biochar fraction present in the soil assuming that the pool of fine fraction is constant. However, fine biochar particles may be created due to the bombardment of fast-moving sand on biochar particles (saltation). Thus, a comprehensive mechanistic understanding of eolian transport including fine biochar particle generation is necessary.

The fundamental mechanisms of biochar emission can be inferred from the processes of dust emission from natural soil surfaces. Depending on the soil particle size and the wind conditions, eolian transport of soil particles can be classified into four non-discrete physical regimes (Figure 1): creep (>500 μm), saltation (70–500 μm), short-term suspension (20–70 μm), and long-term suspension (<20 μm) (Bagnold, 1974; Kok et al., 2012; Ravi et al., 2011). The saltation-induced particle emission, the major driver of dust emissions from natural surfaces, occurs when the wind speed exceeds a minimum threshold velocity (Shao et al., 1993). At wind speeds beyond the threshold velocity, saltation-sized particles are lifted from the ground and carried by wind to short distances as a horizontal flux within the lower 1 m of the atmosphere (Bagnold, 1974). The saltating particles can collide with other particles or aggregates on the surface and generate fine particles (Gillette et al., 1974). The generated particles can be ejected and entrained in the airflow as a vertical flux (Figure 1) (Gillette & Walker, 1977). As biochar could break easily by surface abrasion and compaction (Ghavanloughajar et al., 2020; Le et al., 2020) compared with other soil minerals, the saltation-induced emission could be much higher in biochar-amended soil. However, the effect of saltation on biochar emission has not been investigated.

Compared with saltation, direct suspension at low wind speed is generally considered a minor component of total dust flux in natural soils as the wind speed at the ground surface may not be sufficient to overcome the interparticle forces between fine particles including capillary force (Bagnold, 1974). However, the cohesive force by water film (moisture bonding) between particles is expected to be lower in water-repellent or hydrophobic particles, even under low moisture conditions (Ravi et al., 2006). As biochar surface is more hydrophobic than natural soil (Batista et al., 2018), the cohesive force by surface water film is expected to be much smaller. Furthermore, biochar has a lower density than natural soil minerals, resulting in low gravitational pull against aerodynamic lift. Thus, we hypothesize that a combination of low interparticle forces and

low density could significantly increase biochar particle emission from soils, even at the wind speeds where emission from natural soil is not expected. However, current models for fugitive dust emissions (U.S. EPA, 1995; Loosmore & Hunt, 2000) assume the soil surface to be stable with negligible dust emissions in the absence of transient events such as surface disturbances and wind speeds exceeding the saltation threshold of the soil. Thus, it is critical to evaluate particulate matter emissions from biochar-amended soil at wind speeds below the typical soil threshold values.

Here, we examine the potential of PM_{10} (inhalable particles with diameters less than or equal to 10 µm) emission from biochar-amended soil by direct suspension without saltation at low wind speed and by saltation at high wind speeds. We hypothesize that biochar addition could disproportionally increase fine particle emission from amended soils by preferential emission of fine biochar particles even at wind speeds below the characteristic threshold velocity of the background soil. To test the hypothesis, we estimated changes in PM_{10} emission from sand amended with 0–4% (by weight) biochar with and without fines at different wind speeds in a wind tunnel equipped with sand abraders. We propose a synthetic framework to explain the particulate matter generation and emissions from biochar-amended soils, which can be used to assess the biochar emission potential and its health risks.

2. Materials and Methods

2.1. Soil Media

We used quartz sand (Ottawa 20-30 sand, US Silica, IL, USA) with 97% of its grain sizes within 0.60 to 0.85 mm and commercially available biochar (Confluence Energy, Kremmling, CO, USA) manufactured by slow pyrolysis of pine wood at 300°C. This biochar was selected because woody biomass is currently the largest source (87%) of biochar feedstock for the biochar industry globally (Jirka & Tomlinson, 2015). The air-dried biochar was sieved to create two size fractions: unsieved and sieved (>2 mm). Removal of fine particles in the sieved biochar enabled us to evaluate the contribution of the abrasion of large biochar particles by saltation on biochar emission. Biochar samples were mixed thoroughly with sand to make uniform mixtures containing sieved or unsieved biochar at 1%, 2%, and 4% by weight, which is approximately equivalent to 5%, 10%, and 20% by volume, respectively. The mixtures represent a wide biochar application rate in agricultural and remediation practices (Tang et al., 2013). The biochar-sand mixtures had moisture contents of less than 1% by weight (Table S1).

The particle size distribution of sand was determined using a laser diffraction particle size analyzer, with a measurement range of 0.017 to 2,000 µm (model LS 13 320, Beckman Coulter, Brea, CA, USA). As biochar size can exceed 2 mm, the size distribution of the biochar was determined using an optoelectronic particle size analyzer (model CAMSIZER, Retsch Technology Gmbh, Germany), which determines particle size between 40 to 8,000 µm. The water repellency of sand and biochar was quantified using water drop penetration time, the average time (seconds) required for uniform-sized water drops to penetrate the surface of sand and biochar. The characteristics of sand and biochar are provided in Table S2.

2.2. Wind Tunnel Design

We used a non-recirculating wind tunnel (7.3 m long, 1.0 m wide, and 1.2 m high) at the USDA-ARS Colombia Plateau Air Quality Research (Pullman, WA), which can generate free stream velocities between 2 to 20 ms^{-1}. The test section of this wind tunnel had plexiglass windows and was equipped with removable metal trays ($1 \times 0.2 \times 0.02$ m). The detailed design and operation of the wind tunnel are described elsewhere (Sharratt & Vaddella, 2012).

The wind velocity was measured using pressure transducers connected with a pitot tube installed upwind from the soil tray at six different heights (0.5, 1, 2, 4, 6, and 10 cm) from the soil surface. Saltation was detected using a SENSIT wind eroding mass flux sensor (SENSIT Company, Redlands, CA) (Ravi et al., 2006) mounted in the wind tunnel with the sensitive part at a height of 1 cm from the surface downwind from the soil tray. Dust concentrations were measured immediately downwind of the soil tray using PM_{10} sensors (DustTrak, TSI incorporated, MN) installed at the same incremental heights above the surface as the wind velocity sensors. The sensor locations above ground were chosen based on the boundary layer considerations for the wind tunnel identified in a previous study (Copeland et al., 2009). The ambient laboratory dust was maintained at a low level, and the experiments were carried out at a temperature range of 10–20°C and
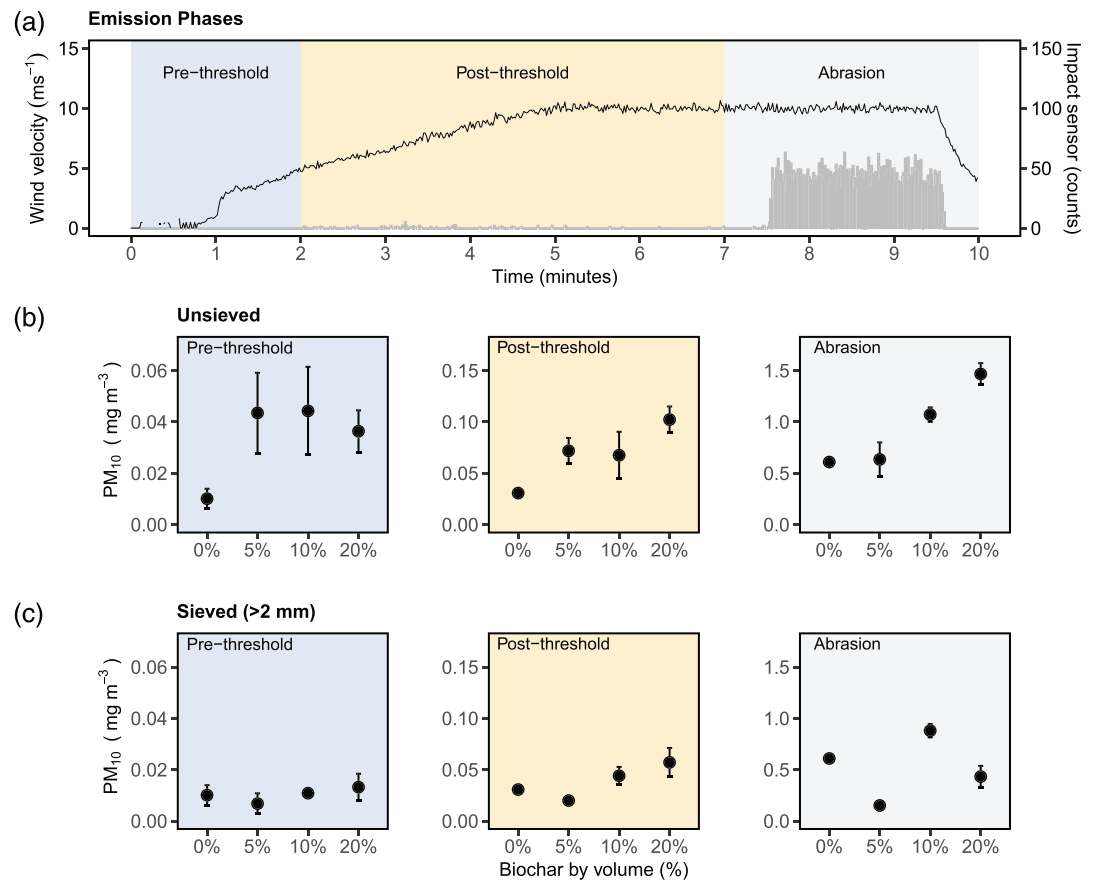
Figure 2. (a) Wind velocities (black line), and saltation activity (gray line) in three experimental phases, and average PM_{10} concentrations (0.5 cm) in three phases from sand amended with (b) unsieved and (c) sieved biochar. The error bars represent one standard deviation over the mean of three replicates.

relative humidity of 40–50%. The experimental parameters were collected every second during the wind tunnel tests.

2.3. Wind Tunnel Experiments

Triplicate tests were conducted for each treatment. Each 10-min wind tunnel test consists of multiple stages (Figure 2a). Initially, the wind velocity was increased stepwise to attain a wind speed just below the threshold value of the soil and then increased slowly until the particle impact sensor indicated particle movement (approximately after 2 min), suggesting that the characteristic threshold velocity was achieved (Figure 2a). The wind speed above the threshold speed was maintained for 5 more minutes. After this period, active saltation characteristic of field conditions was achieved by introducing the same sand as abrader into the air stream of the wind tunnel for 3 more minutes. The approximate abrader rate for this tunnel is around $0.5 \, g \, m^{-1} \, s^{-1}$, which is representative of soil flux during extreme high winds on the Columbia Plateau region (Sharratt & Schillinger, 2014). The saltating and suspended sediments up to a height of 0.75 m above the surface were sampled downwind of the tray using a vertically integrating isokinetic slot sampler (Pi et al., 2018). The particle size distribution of the collected samples was determined using a laser diffraction particle size analyzer (LS 13 320, Beckman Coulter, Brea, CA, USA).

2.4. Calculation of the Threshold Velocity and Wind Profile

Threshold velocity was determined based on the velocity at which the number of particles impacting the sensor (SENSIT) per second abruptly increased (Figure 2a). The threshold velocity was determined only for the three replicates of the control sand, as it was not possible to determine the abrupt change in SENSIT activity for biochar-amended soils. After threshold conditions, constant wind velocity was maintained, and abraders

were released from the upwind of the soil tray. Before the experiment, the velocity values at incremental heights inside the wind tunnel were used to calculate the parameters of the wind profile, including the roughness length (z_m), calculated by fitting the Prandtl-von Karman logarithmic law (log-wind law, Equation 1) to the measured wind speed profile.

$$u(z) = \frac{u_*}{0.4} \ln\left(\frac{z}{z_m}\right) \tag{1}$$

where $u(z)$ is wind velocity at height z, u_* is the shear velocity (or friction velocity), z_m is the aerodynamic roughness length, and 0.4 is the von Karman constant (Campbell & Norman, 1998).

2.5. Calculation of Particulate Matter Emission Rate

To compare net emission rates ($\dot{E}$—mass emitted per unit time) between different treatments, an emission rate was estimated by integrating the product of velocity and PM_{10} concentrations from incremental heights inside the tunnel. We simplified the methodology described by Roney and White (2006), which involves a control volume analysis of inflow and outflow measurements represented as

$$\dot{E} = \frac{1}{L}\int_0^h (c_{out}u_{out} - c_{in}u_{in})\, dz \tag{2}$$

where $\dot{E}$ is the emission rate defined as mass emitted per unit time, L is the length of the soil tray (1 m), c is the PM_{10} average concentration, and u is the average flow velocity of 1-min intervals. The velocity profile in the wind tunnel was typically the same upwind and downwind of the soil tray, and the PM_{10} concentration in the incoming air was found to be very small compared to concentrations downwind during the experiments. Hence, for this analysis, we assumed the inflow term ($c_{in}u_{in}$) to be negligible. After saltation conditions were established (after 2 min), 1-min average PM_{10} concentrations and velocity profiles at different heights were fitted to construct the regression curves. Roney and White (2006) showed that the PM_{10} concentrations typically followed a power law trend, $c = a\, h^{-b}$, where a and b are fitting coefficients. As the declining trend of PM_{10} with height relationship was only valid during periods of active emission from soil surfaces (saltation stage and abrasion stage), the emission rates were calculated only for these stages. The velocity profile was fitted to typical log-wind (law of the wall) profiles $u = c \log(z) + d$, where u is the velocity at height z and c and d are fitting coefficients. To calculate an emission rate per unit area, the coefficients from regression fits were determined, and the product of the concentration and velocity was integrated numerically from 0.05 m to the height at which PM_{10} concentration reaches the background concentration as in Equation 1. This upper height was set to the highest PM_{10} measurement height (0.1 m) for our study. During the post-saltation (2–7 min) and abrasion phases (7–10 min) where the concentration profiles were developed, $\dot{E}$ was calculated for every minute and averaged for that phase. A detailed description of the analysis is provided in Roney and White (2006) and Copeland et al. (2009).

2.6. A Theoretical Framework for Wind Transport of Biochar

Wind erosion of bare soil is often modeled as time-dependent conservation of mass of sources and sinks associated with the erosion and transport in the control volume (Hagen, 1991). Using this framework, the mass conservation of saltating aggregates in a two-dimensional control volume (Figure 1) can be represented as

$$\frac{\partial \overline{Q}h}{\partial t} = -\frac{\partial q_x}{\partial x} - \frac{\partial q_y}{\partial y} + E_{ds} + E_a - E_t - E_{ss} \tag{3}$$

where $\overline{Q}$ is the average concentration of saltating particles in a control volume of height h during time t; q_x is the component of saltation discharge in the x direction; q_y is the component of saltation discharge in the y direction; E_{ds} is the net vertical flux from emission of fine soil particles without saltation; E_a is the flux from abrasion of particles, aggregates, or crust by saltation bombardment; E_t is the particles trapped in the control volume; and E_{ss} is the suspension of fine particles induced by saltation bombardment.

Saltation starts once the wind velocity exceeds the threshold shear velocity (Equation 4), which depends on several factors including wind characteristics, field surface conditions, size and shape of the soil particles, and soil water content (Kok et al., 2012). To demonstrate the effect of density and particle size on
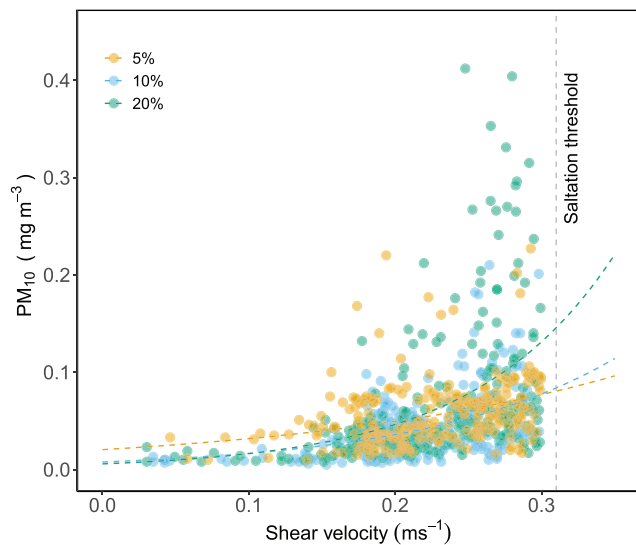
Figure 3. PM_{10} emission from sand mixed with 5%, 10%, or 15% biochar as a function of shear velocity below the threshold shear velocity of the sand. The data are fitted with an exponential model (dashed lines).

threshold shear velocity for dry soil and biochar particles, we adopted a semi-empirical expression for the saltation fluid threshold, u_{*t} (Shao & Lu, 2000).

$$u_{*t} = A_N \sqrt{\frac{\rho_p - \rho_a}{\rho_a} g D_p + \frac{\gamma}{\rho_a D_p}} \qquad (4)$$

where ρ_a is the air density, ρ_p is the particle density, D_p is the particle diameter, g is the acceleration due to gravity, $A_N = 0.11$ is a dimensionless parameter, and γ is a parameter which scales the strength of the interparticle forces. Here we use $\gamma = 2.9 \times 10^{-4}\,\mathrm{Nm^{-1}}$ from Kok and Renno (2006) for loose dust and sand particles.

2.7. Statistical Methods

Statistical tests one-way ANOVA and Tukey's post hoc test were conducted (R version 4.0.0) to test if the PM_{10} emissions from control and treatments were significantly different. A p value below 0.05 is considered significant.

3. Results

3.1. Addition of Biochar Increased Emission

The addition of the unsieved biochar significantly ($p < 0.05$) increased the PM_{10} emission at all concentrations compared to background sand (Figure 2b). Initially, the average PM_{10} concentration measured close to the soil surface (0.5 cm) was more than 4 times the control sand in the pre-threshold stage, indicating higher direct suspension of particulate matter without reaching active saltation condition (Figure 2b). However, the differences in PM_{10} emissions between the different concentrations of unsieved biochar were not significant ($p > 0.05$). At wind speeds above the threshold, PM_{10} emissions were 2–3 times higher than that of background sand with the 20% biochar exhibiting the highest PM_{10} emission. As expected, the overall emission increased in the presence of sand abrader, with PM_{10} emission increasing with an increase in biochar concentration (Figure 2b). The emissions from samples containing 10% and 20% biochar were significantly ($p < 0.05$) different from the samples with 5% biochar and no biochar.

Emissions from sand with sieved biochar (>2-mm fraction) were consistently lower than the emissions from sand with unsieved biochar at all wind conditions (Figure 2c). The PM_{10} emissions from sand with and without biochar were not significantly different in the pre-threshold phase ($p > 0.05$). However, during post-threshold conditions, the PM_{10} concentrations from 10% and 20% biochar treatments were significantly higher ($p < 0.05$) than other treatments. During the abrasion phase, only the 10% biochar treatment showed significantly higher ($p < 0.05$) emissions, while 5% showed significantly lower ($p < 0.05$) emissions compared to the control. This decline in emissions from the 5% biochar treatment could have been due to the lower probability of abraders impacting biochar particles as compared to treatments with higher concentrations of biochar.

3.2. Biochar Emission Occurred Before Threshold Velocity

During the initial phase (<2 min) when fine particles can be suspended without saltation in soils and when supply of fines is not limited (e.g., unsieved biochar treatments), the PM_{10} concentrations increased exponentially with increasing shear velocity (u_*) (Figure 3). The saltation threshold shear velocity of the sand was determined to be 0.32 ms^{-1}.

3.3. Biochar Emission by Saltation

During the post-threshold phase (2–7 min), the average PM_{10} emission rates (E) for the sands amended with unsieved biochar were significantly higher ($p < 0.05$) than sand without biochar (Figure 4a), but in the same condition, the average PM_{10} emission rates from sand with and without sieved biochar were not significantly different ($p > 0.05$). In the post-threshold phase, the average PM_{10} emission rates from the unsieved
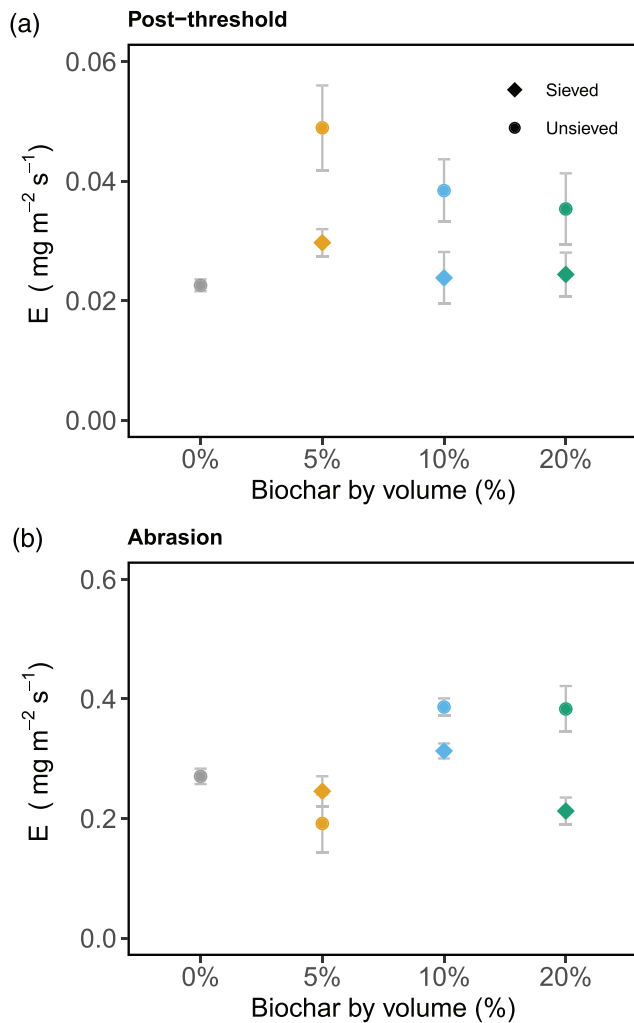
Figure 4. The average PM_{10} emission rate (E) during the post-threshold phase (2–7 min) and abrasion phase (7–10 min) of the wind tunnel experiment.

treatments were significantly higher ($p < 0.05$) compared to sieved treatments, except for the 20% biochar ($p > 0.05$).

In the abrasion phase (7–10 min), the average PM_{10} emission rates from 10% and 20% unsieved biochar treatments were significantly higher ($p < 0.05$) than the control, while the 5% biochar treatment had a significantly lower emission rate ($p < 0.05$) than control (Figure 4b). For sand amended with sieved biochar, samples with 10% biochar had significantly higher ($p < 0.05$) emission rates than the control sand (Figure 4b). The average PM_{10} emission rates from the unsieved treatments were significantly different and higher ($p < 0.05$) compared to sieved treatments, except for the 5% biochar ($p > 0.05$).

3.4. Particle Size Distribution of Sediments

The particle size distribution of the sediments collected in the integrated horizontal slot sampler indicates that the fine particles were generated even from mixtures containing sieved biochar fractions with no particles under 2-mm diameter (Figure 5). Irrespective of biochar size, a secondary peak in biochar size below 500 µm was observed (Figure 5).

4. Discussion

Our results indicate an increase in particulate matter emission from biochar-amended soil by direct suspension in more frequent low wind speed conditions and by abrasion at less frequent higher wind speed conditions. Using the mass conservation approach, we explain how amending soil with biochar can alter particulate matter emission at different wind regimes. Common biochar amendments have lower particle density (ρ_p) ranges of 1,400–2,000 kg m^{-3}, compared to bulk soil particles, which varies between 2,400 and 2,800 kg m^{-3} (Blanco-Canqui, 2017; Brewer et al., 2014). As biochar has a lower density than the bulk soil, a biochar particle would experience less gravitational pull than a sand or soil particle of the same size. Consequently, biochar can be preferentially entrained by wind, even before the characteristic threshold condition for the soil is attained.

Using the Shao and Lu (2000) model (Equation 3), we show that the lower density of biochar particles will result in lower threshold shear velocity and hence higher erodibility (Figure 6). Moreover, biochar particles have been known to have different levels of water repellency or hydrophobicity depending on the source material and the production process, which results in higher air-water contact angles (range from 57° to 132°) (Batista et al., 2018) than typical soil particles (range from 0° to 30°). In dry soils, threshold shear velocity is shown to depend on interparticle forces (Ravi et al., 2006). Thus, the biochar particle with higher contact angles is expected to have weaker interparticle forces and lower threshold velocities. In fact, particle density of biochars manufactured by the slow pyrolysis of wood (300°C), as the one used in our study, is around 1,400 kg m^{-3} (Brewer et al., 2014). The air-dried biochar also showed water repellency (water drop penetration time of 5–10 s), which will weaken the interparticle moisture bonding between particles in the soil matrix (Ravi et al., 2006). Indeed, previous studies have demonstrated the effect of soil water repellency on threshold shear velocity of wind erosion even in air-dried soils, where the surface soil moisture is controlled by air humidity (Ravi et al., 2006).

A previous study (Loosmore & Hunt, 2000) has demonstrated long-term steady dust flux from the soil below threshold conditions in the absence of saltation bombardment and showed that the dust flux (F_d) scales as the third power of the friction velocity ($F_d = 3.6 \, u_*^3$). In our study, the biochar particles may have been preferentially eroded due to their low density and moisture repellent properties. The PM_{10} concentrations were found to be an increasing function of the shear velocity (u_*) when fine particles were not limited (Figure 3). Biochar amendments are often used to improve properties of sandy and sandy loam agricultural soils where
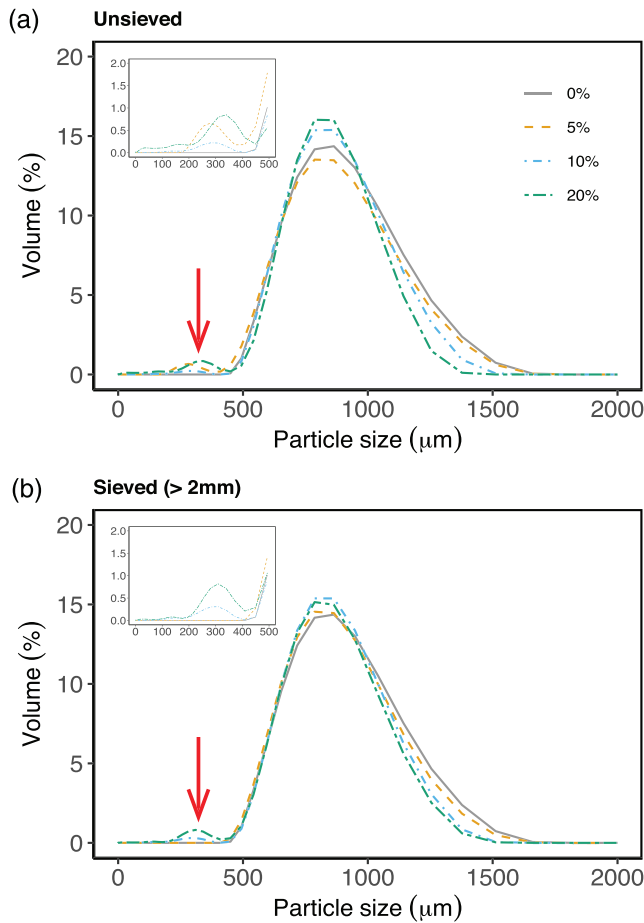
(a) Unsieved

(b) Sieved (> 2mm)

Figure 5. The particle size distribution of samples collected in the horizontally integrated slot sampler. Arrow marks and insets show the peak of fine biochar particles, which was absent in the control sample.
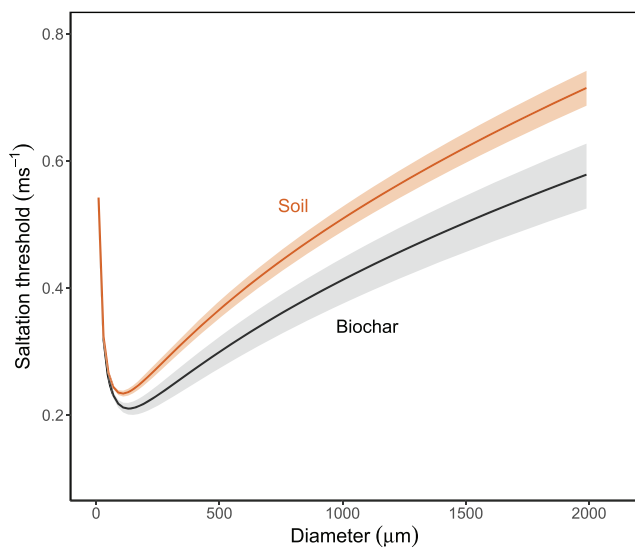

Figure 6. Modeled threshold shear velocity for initiating saltation for soil and biochar particles with different sizes and density ranges. The shaded region indicates density ranges for common biochar amendments and bulk soil particles.

the saltation threshold shear velocities can range from 0.25 to 0.6 ms^{-1} for loose soil and even higher than 1.5 ms^{-1} for crusted conditions (Gillette, 1988). Hence, ample opportunities exist for biochar particles to be directly suspended from these soils before attaining saltation. This is particularly important because wind events below these velocity ranges occur more frequently compared to events exceeding the saltation threshold. Under these conditions, biochar with a high proportion of fine particles or ash content can be re-entrained in air. Even though these dust fluxes are small compared to saltation scenarios, this resuspension could be a significant emission mechanism of biochar particles with sorbed chemical species. Hence, the current approach (e.g., U.S. EPA, 1995) of using saltation threshold conditions as a proxy for initiation of particulate emission from soil surfaces may not be an appropriate parameter for evaluating biochar emission and particle-mediated contaminant transport scenarios in air.

Once the threshold conditions are exceeded, the dominant particulate matter emission mechanism is the surface abrasion of soil particles (Baddock et al., 2013; Shao et al., 1993). The particle emission by abrasion not only depends on the saltation flux, the velocity of the abrader, and the impact angle but also on the properties of the target surfaces including the crushing energy of aggregates or particles (Pi et al., 2020). Biochar application has been found to reduce soil strength and penetration resistance possibly because of the reduction in soil bulk density and increase in total porosity (Busscher et al., 2010; Chan et al., 2007). Biochar addition was also found to decrease cohesion in soil due to the formation of clay-carbon complexes that reduce the cohesive forces between the biochar-amended soil particles compared to carbon-carbon bonding in biochar or clay-clay bonding in soil (Zong et al., 2014). Moreover, the presence of ash in the biochar has negative effects on soil strength and stability (Sadasivam & Reddy, 2015). All these impacts depend upon the physicochemical properties of the biochar, feedstock, and the production process (Yargicoglu et al., 2015). Due to the lower particle density and load-bearing capacity of biochar, the crushing energy of biochar particles (and modulus of rupture) is much lower than typical soil particles (Gümüş et al., 2019). So saltating sand grains colliding with biochar can break biochar particles and generate fine particles. This is particularly significant as biochar is commonly used as a soil amendment to improve nutrient and water retention in sandy textured soils, where the supply of abraders—sand-sized particles for initiating saltation-induced bombardment—is not limited (Gelardi et al., 2019; Ravi et al., 2016). We also acknowledge that fine particle generation is facilitated by other physical and chemical mechanisms of biochar disintegration in soils (Cao et al., 2017; Le et al., 2020; Spokas et al., 2014).

Based on the physical processes involved in eolian transport and the experimental results and theoretical analysis described above, we propose a synthetic framework for particulate matter emissions from biochar-amended soils (Figure 1). At wind velocities lower than the threshold of the soil, fine biochar particles which are lighter than soil particles can be removed constantly by wind. After attaining saltation conditions, biochar particles can be more susceptible to abrasion by sand particles leading to higher emissions of fine particles. Some of these fine particles can be trapped by surface depressions or sheltered by roughness elements on the surface or redeposited by settling. These particles can be the source for

entrainment when wind velocity is below the saltation threshold. So, the sandblasting can generate fines, thereby replenishing the fine particle pools, which can be resuspended during low-velocity conditions. The low-velocity conditions are more frequent or rather continuous compared to event-based saltation activity, thereby the increased risk of air quality deterioration from biochar-amended soil surfaces.

We acknowledge that under field conditions, particulate matter emission by wind can vary with other factors such as soil texture, structure, organic matter, and vegetation cover (Kok et al., 2012; Ravi et al., 2011). For this study, we used air-dried clean sand and biochar to avoid confounding factors in the field that could affect the threshold shear velocity for wind erosion. Further, the threshold shear velocity depends on the moisture content at the soil surface which may undergo significant drying during the wind tunnel experiments using artificially wetted soils. Previous studies using air-dried soils have shown that humidity of the overlying air can control the temporal variability in surface soil moisture and impact interparticle bonding forces (Ravi et al., 2004). This is particularly true for wind erosion-prone arid and semi-arid regions which are often characterized by very low annual precipitation and with scarce vegetation cover, and hence, the variation in surface soil moisture is significantly affected by changes in atmospheric humidity (Ravi et al., 2004). Thus, we expect that the low moisture content (<1% by weight) of sand and biochar mixture used in this study would have affected the interparticle forces.

Our study shows an increased risk of fine particulate emissions from biochar-amended soil in the conditions previously not considered: at low wind speed, which occurs more frequently. Fine particle emission is an emerging health concern because of the potential of biochar-bound contaminants. The biochar-mediated immobilization of heavy metal ions, pesticides, pharmaceuticals, and microbes from the soil is often an intended outcome of biochar application (Bair et al., 2016). Contaminants such as polycyclic aromatic hydrocarbons, heavy metals, dioxins, furans, and polychlorinated biphenyls can be formed or adsorbed in biochar even during biochar production, depending on the feedstock and production temperature (Gelardi et al., 2019; Hale et al., 2012; Yargicoglu et al., 2015). Currently, a wide disparity exists in the concentration of these pollutants in commercial biochar products, which has been attributed to the fewer regulatory standards for biochar contaminant levels in many counties (Gelardi et al., 2019).

5. Conclusion

Overall, this study shows an increased risk of fine biochar emissions and generation from biochar-amended soil in the wind regimes previously not considered: by direct suspension in more frequent low wind speeds and by abrasion at less frequent higher wind speeds. The applied biochar can be transported out of the soil system by wind, potentially along with adsorbed contaminants. Our result indicates that current fugitive dust emission models may underestimate the biochar emission potential from amended soils, as most models (e.g., U.S. EPA, 1995) assume the soil surface to be stable with negligible dust emissions in the absence of surface disturbances or wind speeds exceeding the saltation threshold of the soil. Further, the underlying assumption in many biochar application scenarios about the long-term stability of applied biochar needs to be reevaluated. This study will help assess the wind-driven biochar emission from amended soils and its impact on public health risks.

Conflict of Interest

The authors declare no conflicts of interest relevant to this study. Any use of trade names is for descriptive purposes only and does not imply endorsement of any format.

Data Availability Statement

All data used in our work can be found online (https://figshare.com/s/57adb7debb574b25e3eb).

References

Baddock, M., Boskovic, L., Strong, C., McTainsh, G., Bullard, J., Agranovski, I., & Cropp, R. (2013). Iron-rich nanoparticles formed by aeolian abrasion of desert dune sand. *Geochemistry, Geophysics, Geosystems*, *14*, 3720–3729. https://doi.org/10.1002/ggge.20229
Bagnold, R. (1974). *The physics of blown sand and desert dunes* (1st ed.). Netherlands: Springer. https://doi.org/10.1007/978-94-009-5682-7
Bair, D. A., Mukome, F. N. D., Popova, I. E., Ogunyoku, T. A., Jefferson, A., Wang, D., et al. (2016). Sorption of pharmaceuticals, heavy metals, and herbicides to biochar in the presence of biosolids. *Journal of Environmental Quality*, *45*, 1998–2006. https://doi.org/10.2134/jeq2016.03.0106

Batista, E. M. C. C., Shultz, J., Matos, T. T. S., Fornari, M. R., Ferreira, T. M., Szpoganicz, B., et al. (2018). Effect of surface and porosity of biochar on water holding capacity aiming indirectly at preservation of the Amazon biome. *Scientific Reports*, *8*, 10677. https://doi.org/10.1038/s41598-018-28794-z

Blanco-Canqui, H. (2017). Biochar and soil physical properties. *Soil Science Society of America Journal*, *81*, 687–711. https://doi.org/10.2136/sssaj2017.01.0017

Brewer, C. E., Chuang, V. J., Masiello, C. A., Gonnermann, H., Gao, X., Dugan, B., et al. (2014). New approaches to measuring biochar density and porosity. *Biomass and Bioenergy*, *66*, 176–185. https://doi.org/10.1016/j.biombioe.2014.03.059

Busscher, W. J., Novak, J. M., Evans, D. E., Watts, D. W., Niandou, M. A. S., & Ahmedna, M. (2010). Influence of pecan biochar on physical properties of a Norfolk loamy sand. *Soil Science*, *175*(1), 10–14. https://doi.org/10.1097/SS.0b013e3181cb7f46

Campbell, G. S., & Norman, J. M. (1998). *An introduction to environmental biophysics*. New York, NY: Springer. https://doi.org/10.1007/978-1-4612-1626-1

Cao, T., Chen, W., Yang, T., He, T., Liu, Z., & Meng, J. (2017). Surface characterization of aged biochar incubated in different types of soil. *BioResources*, *12*, 6366–6377.

Cao, X., Ma, L., Gao, B., & Harris, W. (2009). Dairy-manure derived biochar effectively sorbs lead and atrazine. *Environmental Science & Technology*, *43*(9), 3285–3291. https://doi.org/10.1021/es803092k

Chan, K. Y., Van Zwieten, L., Meszaros, I., Downie, A., & Joseph, S. (2007). Agronomic values of greenwaste biochar as a soil amendment. *Soil Research*, *45*(8), 629–634. Retrieved from. https://doi.org/10.1071/SR07109

Copeland, N. S., Sharratt, B. S., Wu, J. Q., Foltz, R. B., & Dooley, J. H. (2009). A wood-strand material for wind erosion control: Effects on total sediment loss, PM_{10} vertical flux, and PM_{10} loss. *Journal of Environmental Quality*, *38*(1), 139–148. https://doi.org/10.2134/jeq2008.0115

Gelardi, D. L., Li, C., & Parikh, S. J. (2019). An emerging environmental concern: Biochar-induced dust emissions and their potentially toxic properties. *Science of the Total Environment*, *678*, 813–820. https://doi.org/10.1016/j.scitotenv.2019.05.007

Genesio, L., Vaccari, F. P., & Miglietta, F. (2016). Black carbon aerosol from biochar threats its negative emission potential. *Global Change Biology*, *22*, 2313–2314. https://doi.org/10.1111/gcb.13254

Ghavanloughajar, M., Valenca, R., Le, H., Rahman, M., Borthakur, A., Ravi, S., et al. (2020). Compaction conditions affect the capacity of biochar-amended sand filters to treat road runoff. *Science of the Total Environment*, *735*, 139180. https://doi.org/10.1016/j.scitotenv.2020.139180

Gillette, D. A. (1988). Threshold friction velocities for dust production for agricultural soils. *Journal of Geophysical Research*, *93*(D10), 12,645–12,662. https://doi.org/10.1029/JD093iD10p12645

Gillette, D. A., Blifford, I. H. Jr., & Fryrear, D. W. (1974). The influence of wind velocity on the size distributions of aerosols generated by the wind erosion of soils. *Journal of Geophysical Research (1896–1977)*, *79*(27), 4068–4075. https://doi.org/10.1029/JC079i027p04068

Gillette, D. A., & Walker, T. R. (1977). Characteristics of airborne particles produced by wind erosion of sandy soil, high plains of West Texas. *Soil Science*, *123*(2), 97–110. https://doi.org/10.1097/00010694-197702000-00004

Gümüş, İ., Negis, H., & Şeker, C. (2019). Influence of biochar applications on modulus of rupture and aggregate stability of the soil possessing crusting problems. *Toprak Su Dergisi*, *8*, 81–86. https://doi.org/10.21657/topraksu.538580

Hagen, L. J. (1991). Wind erosion mechanics: Abrasion of aggregated soil. *Transactions of ASAE*, *34*(3), 831–837. https://doi.org/10.13031/2013.31737

Hale, S. E., Lehmann, J., Rutherford, D., Zimmerman, A. R., Bachmann, R. T., Shitumbanuma, V., et al. (2012). Quantifying the total and bioavailable polycyclic aromatic hydrocarbons and dioxins in biochars. *Environmental Science & Technology*, *46*(5), 2830–2838. https://doi.org/10.1021/es203984k

Janssen, N. A. H., Hoek, G., Simic-Lawson, M., Fischer, P., van Bree, L., ten Brink, H., et al. (2011). Black carbon as an additional indicator of the adverse health effects of airborne particles compared with PM_{10} and $PM_{2.5}$. *Environmental Health Perspectives*, *119*(12), 1691–1699. https://doi.org/10.1289/ehp.1003369

Jirka, S., & Tomlinson, T. (2015). State of the biochar industry 2014: A survey of commercial activity in the biochar sector.

Kok, J. F., Parteli, E. J. R., Michaels, T. I., & Karam, D. B. (2012). The physics of wind-blown sand and dust. *Reports on Progress in Physics*, *75*, 106901. https://doi.org/10.1088/0034-4885/75/10/106901

Kok, J. F., & Renno, N. O. (2006). Enhancement of the emission of mineral dust aerosols by electric forces. *Geophysical Research Letters*, *33*, L19S10. https://doi.org/10.1029/2006GL026284

Le, H., Valenca, R., Ravi, S., Stenstrom, M. K., & Mohanty, S. K. (2020). Size-dependent biochar breaking under compaction: Implications on clogging and pathogen removal in biofilters. *Environmental Pollution*, *266*, 115195. https://doi.org/10.1016/j.envpol.2020.115195

Lehmann, J. (2007). A handful of carbon. *Nature*, *447*(7141), 143–144. https://doi.org/10.1038/447143a

Lehmann, J., Rillig, M. C., Thies, J., Masiello, C. A., Hockaday, W. C., & Crowley, D. (2011). Biochar effects on soil biota—A review. *Soil Biology and Biochemistry*, *43*(9), 1812–1836. https://doi.org/10.1016/j.soilbio.2011.04.022

Lehmann, J. J. S. (Ed) (2015). *Biochar for environmental management: Science, technology and implementation* (2nd ed.). NY: Routledge.

Loosmore, G. A., & Hunt, J. R. (2000). Dust resuspension without saltation. *Journal of Geophysical Research*, *105*(D16), 20,663–20,671. https://doi.org/10.1029/2000JD900271

Mbow, C., Rosenzweig, C., Barioni, L. G., Benton, T. G., Herrero, M., Krishnapillai, M., et al. (2019). Food security. In P. R. Shukla, J. Skea, E. Calvo Buendia, V. Masson-Delmotte, H.-O. Pörtner, D. C. Roberts, P. Zhai, et al. (Eds.), *Climate change and land: An IPCC special report on climate change, desertification, land degradation, sustainable land management, food security, and greenhouse gas fluxes in terrestrial ecosystems*. Geneva, Switzerland: Intergovernmental Panel on Climate Change.

Mohanty, S. K., & Boehm, A. B. (2015). Effect of weathering on mobilization of biochar particles and bacterial removal in a stormwater biofilter. *Water Research*, *85*, 208–215. https://doi.org/10.1016/j.watres.2015.08.026

Nguyen, B. T., & Lehmann, J. (2009). Black carbon decomposition under varying water regimes. *Organic Geochemistry*, *40*(8), 846–853. https://doi.org/10.1016/j.orggeochem.2009.05.004

Pi, H., Huggins, D. R., Webb, N. P., & Sharratt, B. (2020). Comparison of soil-aggregate crushing-energy meters. *Aeolian Research*, *42*, 100559. https://doi.org/10.1016/j.aeolia.2019.100559

Pi, H., Sharratt, B., Schillinger, W. F., Bary, A. I., & Cogger, C. G. (2018). Wind erosion potential of a winter wheat-summer fallow rotation after land application of biosolids. *Aeolian Research*, *32*, 53–59. https://doi.org/10.1016/j.aeolia.2018.01.009

Ravi, S., D'Odorico, P., Breshears, D. D. D., Field, J. P., Goudie, A. S. A. S., Huxman, T. E. T. E., et al. (2011). Aeolian processes and the biosphere. *Reviews of Geophysics*, *49*, RG3001. https://doi.org/10.1029/2010RG000328

Ravi, S., D'Odorico, P., Herbert, B., Zobeck, T., & Over, T. M. (2006). Enhancement of wind erosion by fire-induced water repellency. *Water Resources Research*, *42*, W11422. https://doi.org/10.1029/2006WR004895

Ravi, S., D'Odorico, P., Over, T. M., & Zobeck, T. (2004). On the effect of air humidity on soil susceptibility to wind erosion: The case of air-dry soils. *Geophysical Research Letters*, *31*, L09501. https://doi.org/10.1029/2004GL019485

Ravi, S., Sharratt, B. S., Li, J., Olshevski, S., Meng, Z., & Zhang, J. (2016). Particulate matter emissions from biochar-amended soils as a potential tradeoff to the negative emission potential. *Scientific Reports*, *6*, 35984. https://doi.org/10.1038/srep35984

Roney, J. A., & White, B. R. (2006). Estimating fugitive dust emission rates using an environmental boundary layer wind tunnel. *Atmospheric Environment*, *40*(40), 7668–7685. https://doi.org/10.1016/j.atmosenv.2006.08.015

Rumpel, C., Ba, A., Darboux, F., Chaplot, V., & Planchon, O. (2009). Erosion budget and process selectivity of black carbon at meter scale. *Geoderma*, *154*(1-2), 131–137. https://doi.org/10.1016/j.geoderma.2009.10.006

Sadasivam, B. Y., & Reddy, K. R. (2015). Engineering properties of waste wood-derived biochars and biochar-amended soils. *International Journal of Geotechnical Engineering*, *9*, 521–535. https://doi.org/10.1179/1939787915Y.0000000004

Sasidharan, S., Torkzaban, S., Bradford, S. A., Kookana, R., Page, D., & Cook, P. G. (2016). Transport and retention of bacteria and viruses in biochar-amended sand. *Science of the Total Environment*, *548-549*, 100–109. https://doi.org/10.1016/j.scitotenv.2015.12.126

Shao, Y., Raupach, M. R., & Findlater, P. A. (1993). Effect of saltation bombardment on the entrainment of dust by wind. *Journal of Geophysical Research*, *98*, 12,719–719,726. https://doi.org/10.1029/93JD00396

Shao, Y., & Lu, H. (2000). A simple expression for wind erosion threshold friction velocity. *Journal of Geophysical Research*, *105*(D17), 22,437–22,443. https://doi.org/10.1029/2000JD900304

Sharratt, B., & Schillinger, W. F. (2014). Windblown dust potential from oilseed cropping systems in the Pacific Northwest United States. *Agronomy Journal*, *106*, 1147–1152. https://doi.org/10.2134/agronj13.0384

Sharratt, B. S., & Vaddella, V. K. (2012). Threshold friction velocity of soils within the Columbia Plateau. *Aeolian Research*, *6*, 13–20. https://doi.org/10.1016/j.aeolia.2012.06.002

Smith, P. (2016). Soil carbon sequestration and biochar as negative emission technologies. *Global Change Biology*, *22*, 1315–1324. https://doi.org/10.1111/gcb.13178

Sohi, S. P. (2013). Pyrolysis bioenergy with biochar production—Greater carbon abatement and benefits to soil. *GCB Bioenergy*, *5*, i–iii. https://doi.org/10.1111/gcbb.12057

Spokas, K. A., Novak, J. M., Masiello, C. A., Johnson, M. G., Colosky, E. C., Ippolito, J. A., & Trigo, C. (2014). Physical disintegration of biochar: An overlooked process. *Environmental Science & Technology Letters*, *1*, 326–332. https://doi.org/10.1021/ez500199t

Tang, J., Zhu, W., Kookana, R., & Katayama, A. (2013). Characteristics of biochar and its application in remediation of contaminated soil. *Journal of Bioscience and Bioengineering*, *116*, 653–659. https://doi.org/10.1016/j.jbiosc.2013.05.035

Ulrich, B. A., Im, E. A., Werner, D., & Higgins, C. P. (2015). Biochar and activated carbon for enhanced trace organic contaminant retention in stormwater infiltration systems. *Environmental Science & Technology*, *49*, 6222–6230. https://doi.org/10.1021/acs.est.5b00376

United Nations Convention to Combat Desertification. (2009). Required policy actions to include carbon contained in soils including the use of biochar (charcoal) to replenish soil carbon pools, and restore soil fertility and sequester CO_2. In *5th Session of the Ad Hoc Working Group on Long-term Cooperative Action under the Convention (AWG-LCA 5)*. Bonn, Germany.

United States Environmental Protection Agency (U.S. EPA) (1995). Stationary point and area sources. In *Compilation of air pollutant emission factors AP-42* (Vol. 1, 5th ed.). Research Triangle Park, NC: U.S. E.P.A. Office of Air Quality Planning and Standards.

Wang, D., Zhang, W., Hao, X., & Zhou, D. (2013). Transport of biochar particles in saturated granular media: Effects of pyrolysis temperature and particle size. *Environmental Science and Technology*, *47*, 821–828. https://doi.org/10.1021/es303794d

Woolf, D., Amonette, J. E., Street-Perrott, F. A., Lehmann, J., & Joseph, S. (2010). Sustainable biochar to mitigate global climate change. *Nature Communications*, *1*, 56. https://doi.org/10.1038/ncomms1053

Yargicoglu, E. N., Sadasivam, B. Y., Reddy, K. R., & Spokas, K. (2015). Physical and chemical characterization of waste wood derived biochars. *Waste Management*, *36*, 256–268. https://doi.org/10.1016/j.wasman.2014.10.029

Zong, Y., Chen, D., & Lu, S. (2014). Impact of biochars on swell-shrinkage behavior, mechanical strength, and surface cracking of clayey soil. *Journal of Plant Nutrition and Soil Science*, *177*, 920–926. https://doi.org/10.1002/jpln.201300596